

On the low energy properties of fermions with singular interactions

B. L. Altshuler

Department of Physics, MIT, Cambridge, MA 02139

L. B. Ioffe

*Department of Physics, Rutgers University, Piscataway, NJ 08855
and Landau Institute for Theoretical Physics, Moscow, Russia*

A. J. Millis

AT&T Bell Laboratories, Murray Hill, NJ 07974

We calculate the fermion Green function and particle-hole susceptibilities for a degenerate two-dimensional fermion system with a singular gauge interaction. We show that this is a strong coupling problem, with no small parameter other than the fermion spin degeneracy, N . We consider two interactions, one arising in the context of the $t - J$ model and the other in the theory of half-filled Landau level. For the fermion self energy we show in contrast to previous claims that the qualitative behavior found in the leading order of perturbation theory is preserved to all orders in the interaction. The susceptibility χ_Q at a general wavevector $\mathbf{Q} \neq 2\mathbf{p}_F$ retains the fermi-liquid form. However the $2p_F$ susceptibility χ_{2p_F} either diverges as $T \rightarrow 0$ or remains finite but with nonanalytic wavevector, frequency and temperature dependence. We express our results in the language of recently discussed scaling theories, give the fixed-point action, and show that at this fixed point the fermion-gauge-field interaction is marginal in $d = 2$, but irrelevant at low energies in $d \geq 2$.

I. INTRODUCTION

The problem of fermions in two dimensions interacting with a singular gauge interaction has arisen recently in two physical contexts. One is the “gauge theory” approach^{1,2} to the $t - J$ model which has been argued^{3,4} to contain the essential physics of high T_c superconductors. The other is the theory of the half-filled Landau level^{5,6}. In both cases one is led to the theoretical problem of a degenerate Fermi gas interacting with a gauge field characterized by the propagator $D(\omega, k) \sim (\frac{|\omega|}{k} + |k|^{1+x})^{-1}$. This notation is conventional; $x = 1$ in the $t - J$ model case¹ and, because of the unscreened Coulomb interaction, $x = 0$ in the $\nu = 1/2$ case considered by previous authors^{5,6}. If the Coulomb interaction in two dimensions were screened, e.g. by a metallic gate, the model with $x = 1$ would apply even to the $\nu = 1/2$ case. The three dimensional version of this model with $x = 1$ was shown by Reizer⁷ to describe electrons in metals interacting magnetically via a current-current interaction. The highly singular behavior of the gauge propagator at small ω, k complicates the analysis of the theory and has led to conflicting claims in the literature. In this paper we present what we believe is a correct treatment of the low energy properties of the theory.

We study fermions interacting with a gauge field \mathbf{a} , and also with each other via a short range interaction W . We assume the simplest form of the interaction with the gauge field allowed by gauge invariance¹:

$$H = \sum_{p,\sigma} c_{p\sigma}^\dagger \epsilon(p) c_{p\sigma} + \sum_{p,k,\sigma} c_{p+k/2,\sigma}^\dagger \mathbf{a}_k \mathbf{v}(p) c_{p-k/2,\sigma}$$

$$+ \sum_{p_i} W c_{p_1,\alpha}^\dagger c_{p_2,\alpha} c_{p_3,\sigma}^\dagger c_{p_4,\sigma} \delta(\sum p_i) + \frac{1}{4g_0^2} f_{\mu\nu}^2 \quad (1)$$

where we omitted higher order terms in the gauge field \mathbf{a} which lead to less infra-red singular effects. Here, as usual, $f_{\mu\nu} = \partial_\mu a_\nu - \partial_\nu a_\mu$, g_0 is the bare fermion-gauge field interaction constant, $\sigma = 1..N$ is a spin index and $\mathbf{v} = \frac{\partial \epsilon}{\partial \mathbf{p}}$. The $f_{\mu\nu}^2$ term comes from integrating out high energy processes. In the $t - J$ model the spin degeneracy $N = 2$; however, it will be convenient to consider general values of N because the limits $N \rightarrow 0$ and $N \rightarrow \infty$ are solvable. Indeed, as we shall see N is the only expansion parameter of the model.

In the $t - J$ model the fermion operators $c_{p,\sigma}^\dagger$ create “spinons” which are chargeless, spin $1/2$ quanta. Because the spinons have no charge, there is no long-range Coulomb term in W . In this representation the charge is carried by different, spinless quanta which obey Bose statistics (“holons”); we shall not consider their properties in this paper. The Hamiltonian (1) describes the magnetic properties of the “spin-liquid” state of $t - J$ model. For a more detailed discussion of the physical situations to which this model may apply, see, e.g., the review paper by Lee⁸.

In the $\nu = 1/2$ case the spin degeneracy $N = 1$ and one must add to the Hamiltonian (1) additional terms containing the Coulomb interaction and Chern-Simons term. This changes the k^2 term in gauge propagator to $|k|$; the effects of this change will be discussed below in Section IV. Other authors⁹ have found it convenient to consider a continuously varying exponent $|k|^{1+x}$; we find

that the behavior for all $x > 0$ is the same as that for $x = 1$ except for minor changes in exponents. The $x = 0$ case is exceptional because there a controlled expansion for the infrared behavior exists for any N . We give results for general $x > 0$ in Section V. For the rest of this Section we explicitly consider only the “spin liquid” case.

Treating the fermion-gauge field interaction in (1) by perturbation theory leads immediately to two effects. Dressing the gauge propagator by a particle-hole bubble leads to the propagator

$$D(\omega, k) = \frac{1}{\frac{Np_0|\omega|}{2\pi|k|} + \frac{1}{N^{1/2}g^2}k^2} \quad (2)$$

Here the first term in the denominator is due to Landau damping of the gauge field, and p_0 is the curvature of the Fermi surface at the point where the normal to the fermi surface is perpendicular to \mathbf{k} . The second term in the denominator has contributions from the $f_{\mu\eta}^2$ term in the effective action and from the fermion diamagnetic susceptibility; in this term we have redefined the interaction constant g^2 so that the characteristic energy scale remains finite in the limits $N \rightarrow \infty$ and $N \rightarrow 0$ which we consider below.

Using the gauge field propagator to calculate the fermion self energy Σ in the first order of the perturbation theory one finds¹⁰

$$\Sigma^{(1)}(\epsilon) = -i \left| \frac{\omega_0}{\epsilon} \right|^{1/3} \epsilon \quad (3)$$

where the energy scale ω_0 is defined in terms of g, p_0 and the fermi velocity v_F via

$$\omega_0 = \left(\frac{1}{2\sqrt{3}} \right)^3 \frac{2v_F^3 g^4}{\pi^2 p_0} \quad (4)$$

For high- T_c materials ($N = 2$) g^2 was estimated to be $6\sqrt{2}\pi m$ (where m is the fermion mass). This leads to $\omega_0 \sim 500 K$ if the fermion bandwidth is of the order of $2J$.

The dramatic effects found in the leading order of perturbation theory lead one to question whether the perturbation theory makes sense. Several different treatments have appeared^{9,11–14}. The appearance of N in the denominator of the gauge field propagator (2) suggests that the theory should have a tractable $N \rightarrow \infty$ limit and that a $1/N$ expansion about this limit is well behaved. The $N \rightarrow \infty$ limit and the leading $1/N$ corrections to the fermion propagator have been studied by Ioffe and Larkin¹, by Reizer⁷ and by Lee¹⁰ but the higher order corrections and the issue of convergence of the expansion have not to our knowledge been previously examined. We present this analysis in Section II of this paper. We find that the $1/N$ expansion is indeed well defined and the leading order results are qualitatively correct for all physical quantities *except* the $2p_F$ susceptibilities, which acquire additional non-analytic power law dependences with exponents which vanish as $N \rightarrow \infty$.

In order to explain the idea of the analysis we need to introduce some notation and establish typical values of momenta and energies involved in virtual processes. The typical momentum k_ω transferred in a low energy process affecting a fermion with energy ω and momentum p is found from the gauge field propagator, eq. (2), to be

$$k_\omega = N^{1/2} \left(\frac{p_0 g^2 \omega}{\pi} \right)^{1/3}. \quad (5)$$

It is convenient to choose Cartesian coordinates in momentum space so that k_\perp is the change of the momentum of the fermion along the Fermi surface (i.e. perpendicular to \mathbf{p}) and k_\parallel perpendicular to the fermi surface (i.e. along \mathbf{p}). At low energies $k_\parallel \sim |\omega - \Sigma(\omega)|/v_F$ becomes much less than k_\perp which is determined by the gauge field propagator (2), i.e. $k_\perp \sim k_\omega$.

Qualitatively the small value of the higher order corrections at large N can be attributed to a comparatively large typical momentum transfer (5) in this limit as follows. In a typical virtual process fermion probes only a small patch of the Fermi surface of the order of k_ω . The curvature of this piece of the Fermi surface is important if the change in the fermion energy induced in such a virtual process ($v_F k_\perp^2 / (2p_0)$) is large compared with the imaginary part of its self energy (3). Comparing the two we find

$$\frac{v_F k_\epsilon^2}{2p_0 \Sigma^{(1)}(\epsilon)} \sim N \quad (6)$$

Thus, in the limit of large N the curvature of the Fermi surface becomes important and we expect that the scattering becomes essentially two dimensional. In this case the usual phase space arguments¹⁵ show that all crossing diagrams are small in $1/N$, so that a $1/N$ expansion is possible.

An alternative solvable limit, namely $N \rightarrow 0$, was pointed out by Ioffe, Lidsky and Altshuler¹¹. In this limit the curvature of the Fermi surface becomes unimportant and the terms proportional to k_\perp^2 in the denominators of the fermion Green function are negligible. When these terms are dropped the Green function does not depend on k_\perp , which enters only via the propagator of the gauge field (2). Thus, in any diagram one can integrate independently all the gauge field propagators over k_\perp . The gauge field propagator becomes

$$D^{(1D)}(\omega) = \int D(\omega, k)(dk_\perp) = \frac{\tilde{g}}{v_F |\omega|^{1/3}} \quad (7)$$

where $\tilde{g} = \frac{2}{3\sqrt{3}} v_F (2\pi g^4 / p_0)^{1/3} = \frac{4\pi}{3} \omega_0^{1/3}$ is the effective interaction constant. Note that k_\parallel does not appear because it is negligible relative to ω for the reason given below eq. (5).

After these transformations diagrams which do not contain fermion loops (except for those loops implicit in the gauge-field propagator) become the same as in a

1D theory with a retarded interaction given by (7) and the diagrams which contain loops are negligible. Therefore, in the limit $N \rightarrow 0$ the theory can be solved by bosonization methods. Moreover, by reproducing this solution using the diagram technique we find that one dimensional results depend crucially on the exact cancellations specific to 1D models and that at any $N \neq 0$ these cancellations are not exact. These observations allow us to obtain some information about the behavior at $N \ll 1$. The analysis of $N \rightarrow 0$ limit is given in Section III. The solution at $N \rightarrow 0$ turns out to be very similar to the results for the fermion propagator obtained by Khveschenko and Stamp¹⁴ via eikonal methods and by Kwon, Marston and Houghton¹² via a two dimensional bosonization. From our results we see that these calculations are only valid in the strict $N \rightarrow 0$ limit, so that the claim of these authors to have calculated the low energy behavior exactly at $N = 2$ or for the half-filled Landau level is in disagreement with our results.

A third theoretical approach involves scaling equations constructed by eliminating high energy degrees of freedom. J. Gan and E. Wong¹³ derived an action for the gauge field alone by integrating out the fermion degrees of freedom in Hamiltonian (1) and then showed that this action has an infra-red stable weak coupling fixed point in 2 spatial dimensions. From this they concluded that Eq. (2) gives the correct asymptotic form of the gauge field propagator. Kwon et al¹² obtained the same result via bosonisation. Our results for finite N imply that “correct asymptotic form” means that the scaling $\omega \sim q^3$ is preserved, as is the behavior in the limits $k \gg k_\omega$ and $k \ll k_\omega$, but not the precise functional form when $k \sim k_\omega$. An alternative scaling treatment was given by Nayak and Wilczek⁹, extending previous work of Shankar¹⁶ on short range interactions. Nayak and Wilczek wrote a scaling relation for an action based directly on Eq. (1). They concluded that for the $\nu = 1/2$ problem in $d = 2$ the fermion gauge field interaction is marginal and in the “spin liquid” case it is relevant, so that no statements can be made until the strong coupling fixed point is found. However, our results imply that the strong coupling fixed point has a straightforward interpretation: in the “spin liquid” case in d spatial dimensions the bare scaling $\epsilon \sim vk \sim v_F k_\perp^2 / (2p_0)$ is replaced by the new scaling $\epsilon^{d/3} \sim v_F k_\parallel \sim v_F k_\perp^2 / (2p_0)$ found from the leading order gauge field corrections to the fermion propagator. In $d > 2$ we show that any additional corrections from the fermion-gauge-field interactions are irrelevant. In $d = 2$ we show that the corrections are marginal at $x > 0$ and lead to new power laws only in the $2p_F$ susceptibilities. In the case of half-filled Landau level ($x = 0$) these power laws are replaced by a much weaker singularity. For the case of the half-filled Landau level with unscreened Coulomb interaction our results amount to a justification of the leading-order approach of Halperin et. al.⁵. The interpretation of our results in terms of scaling theory is discussed in Section V.

Section VI is a conclusion in which the physical interpretation of our results is discussed.

After this manuscript was completed we learned of two preprints reporting results very similar to some of those reported here. Kim, Furusaki, Wen and Lee¹⁷ calculated particle-hole bubbles at small q to order $1/N^2$ in the spin liquid model, finding, as we did, that the fermi liquid form is not modified by the gauge interaction. Polchinski¹⁸ performed a scaling analysis of the large- N spin liquid model and concluded, as do we, that the curvature of the fermi surface is important and that Migdal-type arguments justify the results of the leading order perturbation theory calculation. He also obtained our result, eq. (27), for the renormalization of the $2p_F$ component of the four fermion interaction.

II. LARGE N LIMIT

This section will show that in the limit $N \rightarrow \infty$ the leading contribution is given by the diagrams with the minimal number of crossings; this will allow us to construct a perturbative series in $1/N$ and obtain physical results in the leading orders of this expansion. We find that to all orders in the expansion the self energy remains proportional to $\epsilon^{2/3}$, that all particle-hole susceptibilities except those at $|\mathbf{Q}| = 2p_F$ retain the usual Fermi liquid form and that correlators at $2p_F$ momentum transfer acquire an anomalous power law dependence.

In order to develop a consistent large N expansion for the Hamiltonian (1) we must take $N \rightarrow \infty$ limit so that the interaction parameter g^2 in (2) remains constant. At $N = \infty$ the only diagrams that survive are the RPA bubble graphs shown in Fig. 1. These bubbles screen the $1/k^2$ behavior of the gauge field. Because the gauge field is transverse, it is not completely screened and the result is Eq. (2).

We now consider the $1/N$ corrections to the fermion propagator. These are shown diagrammatically in Fig. 2. The self energy appearing in the leading diagram (Fig. 2a) was given in Eq. (3). One sees that at energies less than ω_0 or length scales longer than v_F/ω_0 , the self energy becomes larger than the inverse of the bare Green function. We have chosen the way the limit $N \rightarrow \infty$ is taken so that the scale ω_0 remains constant. Because the first correction is of the order of 1 and not of $1/N$, care is required in carrying the $1/N$ expansion to higher orders.

Now consider the $O(1/N^2)$ terms. The first of these (Fig. 2b) scales as $[\Sigma^{(1)}(\epsilon)]^2 / \epsilon \sim \epsilon^{1/3}$. Direct calculation using bare fermion propagators shows that the second term (Fig. 2c) scales as ϵ (up to logarithms). Specifically:

$$\Sigma_b^2(\epsilon, p_\parallel) = \frac{c}{(2\pi)^2 N^2} (i\epsilon - v_F p_\parallel) \left(\ln \frac{\epsilon^{2/3} \omega_0^{1/3}}{|\epsilon + i v_F p_\parallel|} \right)^2 \quad (8)$$

where $c \approx 3.28$ and $p_\parallel = |p| - p_F$. This shows that in the low energy limit the self energy is more singular than

the vertex correction and should be summed first. To calculate to higher order in the $1/N$ expansion we should therefore use the Green function $G^{(1)}$ given by

$$G^{(1)}(\epsilon, \mathbf{p}) = \frac{1}{i\epsilon - v_F p - \Sigma^{(1)}(\epsilon)}, \quad (9)$$

with the self energy $\Sigma^{(1)}(\epsilon)$ is given by (3). In fact this $G^{(1)}$ solves the self-consistent Eliashberg equation $\Sigma = \int DG$ also, because $\Sigma^{(1)}(\epsilon)$ is momentum independent¹⁵. Therefore, the rainbow graphs have been summed and we need only to consider graphs with crossed lines such as shown in Fig. 2c.

Returning now to the vertex corrections we reevaluate the leading vertex correction, shown in Fig. 3a, using (9) for the fermion Green functions. We find that this correction is at most of the order of the bare vertex, moreover, it is of order $(\ln[N]/N)^2$ for external momenta of order k_ω . Explicitly, we find

$$\begin{aligned} \Sigma^{(2)}(\epsilon, p) &= v_F^4 \sum_{\omega_1, \omega_2} \int G^{(1)}(\epsilon + \omega_1, p + k_1) G^{(1)}(\epsilon + \omega_2, p + k_2) G^{(1)}(\epsilon + \omega_1 + \omega_2, p + k_1 + k_2) \\ &\quad \times D(\omega_1, k_1) D(\omega_2, k_2) (d^2 k_1 d^3 K_2) \end{aligned} \quad (11)$$

In order to evaluate (11) we integrate over the parallel components of the momenta $k_{1\parallel}$ and $k_{2\parallel}$ obtaining:

$$\Sigma^{(2)}(\epsilon, p_{\parallel}) = v_F^2 \sum'_{\omega_1, \omega_2} \int \frac{D(\omega_1, k_{\perp 1}) D(\omega_2, k_{\perp 2}) (dk_{\perp 1} dk_{\perp 2})}{A + \frac{v_F}{p_0} k_{\perp 1} k_{\perp 2}} \quad (12)$$

where the prime means that the sum over frequencies is restricted to the region where $\omega_1 + \omega_2 + \epsilon$ has sign opposite to $\omega_1 + \epsilon$ and $\omega_2 + \epsilon$ and

$$A(\omega_1, \omega_2, p_{\parallel}) = v_F p_{\parallel} + i\omega_0^{1/3} \left(|\epsilon + \omega_1 + \omega_2|^{2/3} + |\epsilon + \omega_1|^{2/3} + |\epsilon + \omega_2|^{2/3} \right) \quad (13)$$

Clearly, the second order contribution to the self energy is at most of the order of $1/N$ because it contains $1/N^2$ coming from two gauge propagators and N from the phase volume (note that $k_\omega \propto N^{1/2}$). In fact, the coefficient of the $1/N$ term vanishes because the expression under the integral in (12) is odd in $k_{1\perp}$ and $k_{2\perp}$ and the leading behavior turns out to be

$$\Sigma^{(2)}(\epsilon, p_{\parallel} = 0) = -ic' \left(\frac{\ln N}{4\pi N} \right)^2 \epsilon \left| \frac{\omega_0}{\epsilon} \right|^{1/3}, \quad c' \approx 2.16 \quad (14)$$

The reason for the powers of $1/N$ is essentially that the phase volume available for the process when all three electron lines are on the mass shell is negligible as in the usual Migdal arguments¹⁵, although here the phase volume is small only in $1/N$. Note that the non-zero curvature of the Fermi surface is essential to the argument. Note also that in spatial dimension $d > 2$ the leading self energy is $\epsilon^{d/3}$ so that at any N the small parameter of the ‘‘Migdal expansion’’ is $\epsilon^{\frac{d-2}{3}}$. This is related to the fact, to be discussed at greater length in Section V, that the

$$\begin{aligned} \Gamma_{p,0}^{(1R)}(\omega, q) &= \frac{\sqrt{3}v_F}{\pi} F \left[2^{1/3} \sqrt{3} \pi N \frac{q_{\perp}}{k_{\omega}} \right] \\ F(x) &= \frac{2^{1/3} 3}{4} \frac{1}{x^2} \ln^2 \left(\frac{1}{x} \right) \quad x \gg 1 \\ F(x) &= 0.9422 \quad x = 0 \end{aligned} \quad (10)$$

Qualitatively, the small value of the vertex correction at large N can be attributed to the argument underlying the Migdal theorem in the electron-phonon problem¹⁵, namely that the ‘‘velocity’’ of the boson is much less than the ‘‘velocity’’ of the electron (by ‘‘velocity’’ in the present case we mean $\omega/|k|$). However, the argument is more subtle than in the electron-phonon problem because here we have only small angle scattering. To understand how the argument goes, consider again the second order crossed graph for the self energy Fig. 2c, using now (9) for the fermion Green function.

interaction is marginal in $d = 2$ and irrelevant in $d > 2$. Note that although $\Sigma^{(2)}$ has the same form as $\Sigma^{(1)}$ in the limit $\omega_0^{1/3} |\epsilon|^{2/3} \gg v_F p_{\parallel}$ it does not have exactly the same functional form for $\omega_0^{1/3} |\epsilon|^{2/3} \sim v_F p_{\parallel}$.

Thus, at $N \gg 1$ all diagrams can be classified by the number of crossings and the sets of diagrams with minimal number of crossings should be summed first, a procedure well known from localization theory¹⁹. The result of this summation shows that such diagrams indeed give the leading contributions to the higher order terms of the perturbation expansion but these contributions are not sufficiently singular at low energies and contain extra powers of $1/N$. We discuss the calculations leading to this conclusion in Appendix B.

The absence of low energy singularities in the higher orders of the perturbation theory implies that the results obtained in the leading order are modified only slightly by higher order terms.

The discussion so far has shown that the $1/N$ expansion is well defined and has established the qualitative form of the fermion propagator. Now we verify that higher order corrections in $1/N$ do not change the qual-

itative form of the gauge field propagator. This follows from the general considerations of Gan and Wong¹³, but we believe an explicit derivation is valuable because the validity of the approach of Gan and Wong (which involved integrating out gapless fermions and dealing with an action involving the gauge field only) may be questioned and because the derivation makes clear that al-

though the two limits ($k \gg k_\omega$ and $k \ll k_\omega$) are correctly given by Eq. (2), the precise form for $k \sim k_\omega$ is changed by higher order diagrams.

We first consider the leading term $D^{(R)-1}(\omega, q)$, which is obtained by evaluating the polarization bubble (Fig 1) but with renormalized fermion propagators. This may be written

$$D^{(R)-1}(\omega, q) = \sum_{\epsilon, p} \frac{1}{i\omega_0^{1/3}|\epsilon + \omega|^{2/3} - v_F p_{\parallel} - \frac{v_F}{2p_0}(p_{\perp} + q)^2} \frac{1}{i\omega_0^{1/3}|\epsilon + \omega|^{2/3} - v_F p_{\parallel} - \frac{v_F}{2p_0}p_{\perp}^2} \quad (15)$$

This may be most easily evaluated by subtracting and adding the bare bubble obtained using bare Green functions in (15). In the difference term one may integrate over p_{\parallel} first, then sum over ϵ . The result is

$$D_{(R)}^{-1}(\omega, q) - D^{-1}(\omega, q) \sim \frac{p_0 \omega_0^{1/3} |\omega|^{5/3}}{v_F q^2} \quad (16)$$

Thus, for $|\omega| \ll \omega_0^{-1/2}(v_F q)^{3/2}$, the full propagator is still of the bare form (2). Further, we only need this propagator for $\omega \sim N^{-3/2} g^{-2} p_0^{-1} q^3 \ll \omega_0^{-1/2}(v_F q)^{3/2}$. Thus, the only effect of using renormalized Green functions is to reduce the upper frequency cutoff (which enters no physically interesting result) from vq to $\omega_0^{-1/2}(v_F q)^{3/2}$. A very similar calculation shows that $1/N$ vertex correction to the polarization bubble shown in Fig.4a is of the same order as the self energy correction to the bubble, i.e.:

$$\delta D(\omega, q) \sim \frac{p_0 \omega_0^{1/3} |\omega|^{5/3}}{v_F q^2} \quad (17)$$

Thus, for ω less than the upper cutoff $\omega_0^{-1/2}(v_F q)^{3/2}$ the renormalization of the gauge field propagator is small. In particular, for $q \sim k_\omega$ it is smaller than the bare part by a factor of order of q . However, the two loop diagram, Fig. 4b, leads to a correction which is of the same order as the leading diagrams (Fig. 1) in the infrared limit. We do not discuss the details of the evaluation here (except to note that the dominant contribution comes when the internal gauge-field momentum q is almost parallel to the external momentum, k , and that the fermion loop vanishes if the external frequency $\omega = 0$ but are of the order of unity if $k \sim k_\omega$). This diagram therefore does not change the scaling or the asymptotic forms in the limits $k \gg k_\omega$ or $k \ll k_\omega$ but does change the detailed ω, k dependence of $D(\omega, k)$. This discussion also shows that in general the long wave susceptibilities preserve the Fermi liquid form for small frequencies.

So far we have discussed the effects of gauge fields on the long wave properties of fermions. Now we turn to the effects of gauge field on the fermion vertices with large momentum transfer. The corrections to the vertex with large but arbitrary momentum transfer $|\mathbf{q}| \sim p_F$ are generally small because of the small phase volume available

for virtual processes which leave both fermions with momentum transfer $\mathbf{p} + \mathbf{q} + \mathbf{k}$ and $\mathbf{p} + \mathbf{k}$ close to the Fermi surface. The situation changes only for $|q|$ close $2p_F$. In this case a virtual process with momentum transfer \mathbf{q} along the Fermi surface leaves both fermions with momenta $\mathbf{p} + \mathbf{q} + \mathbf{k}$ and $\mathbf{p} + \mathbf{k}$ near the Fermi surface.

The leading contribution in $1/N$ to the fermion vertex Γ_Q is logarithmically divergent at $Q = 2p_F$; we find that higher powers of N contain higher powers of logarithms; we sum these logarithms using a renormalization group method and find power law singularities in Γ_{2p_F} . These singularities imply that the calculation of the particle-hole susceptibility must be reconsidered. Finally, a singular susceptibility near $2p_F$ may be further modified by the short range four fermion interaction; therefore we must consider also the renormalization of this interaction by the gauge fields.

We begin with the diagrams for Γ_Q shown in Fig. 5. The diagrams shown there diverge logarithmically if all external momenta are on the Fermi surface, external energies are zero and the momentum transfer is exactly $Q = 2p_F$. Since the energy only enters the Green function via $\omega_0^{1/3}|\epsilon|^{2/3}$, the momentum component across the Fermi surface via $v_F k_{\parallel}$ and the momentum along the Fermi surface via k_{\perp}^2 , the divergence is cut off by the largest among

$$\epsilon, \quad \epsilon_{\parallel} = \frac{(v_F k_{\parallel})^{3/2}}{\omega_0^{1/2}}, \quad \epsilon_{\perp} = \frac{k_{\perp}^3/m^{3/2}}{\omega_0^{1/2}}. \quad (18)$$

If, say, the largest is the external frequency we evaluate the diagrams in Fig. 5 and get

$$\delta \Gamma_{2p_F}(\omega) = \left(\frac{1}{2N} + \frac{1}{2\pi^2 N^2} \ln^3(N) \right) \ln \left(\frac{1}{\omega} \right) \Gamma_{2p_F}^0 \quad (19)$$

where $\Gamma_{p_F}^0$ is the bare vertex at small scales or large frequencies. The logarithmic nature of the corrections to the effective interaction allows us to sum higher orders of the perturbation theory by constructing the renormalization group equation:

$$\frac{d\Gamma_{2p_F}}{d \ln(1/\omega)} = \left(\frac{1}{2N} + \frac{1}{2\pi^2 N^2} \ln^3(N) \right) \Gamma_{2p_F} \quad (20)$$

From (20) we see that the vertex grows at large scales as

$$\Gamma_{2p_F}^R \sim \left(\frac{\epsilon_F}{\omega}\right)^\sigma \Gamma_{2p_F}^0 \quad (21)$$

$$\sigma = \frac{1}{2N} + \frac{1}{2\pi^2 N^2} \ln^3(N) + O\left(\frac{1}{N^2}\right) \quad (22)$$

Here we used energy ω for the infra-red cut off assuming that it sets the largest scale among ω , ϵ , ϵ_{\parallel} , ϵ_{\perp} . The result (21) is derived using a large N expansion. It is also of interest to evaluate these diagrams at $N = 2$. The leading order diagram gives $\sigma = 0.25$; the sum of the diagrams shown in Fig. 5b and d gives $\sigma = 0.35$.

The power law growth of the vertex at $2p_F$ distinguishes fermions with a gauge interaction from an ordinary Fermi liquid with short range repulsion and leads to

$$\Pi(\omega, q) = \int G(\epsilon + \omega/2, p + q/2) G(\epsilon - \omega/2, p - q/2) [\Gamma_{\epsilon, p}^{(R)}(\omega, q)]^2 (dp d\epsilon) \quad (23)$$

To evaluate the integral in (23) we note that the main contribution to it comes from the range of momenta and energies related by $\epsilon \sim \epsilon_{\parallel} \sim \epsilon_{\perp} \sim \omega$ (18). Estimating the result by power counting we find that if $\sigma < 1/3$ (as occurs for large N) the integral (23) converges, but if $\sigma > 1/3$ it diverges at $\omega = 0$, $q = 2p_F$. We evaluate the integral in these cases separately and find:

$$\Pi(\omega, q) = \Pi_0 - \sqrt{\frac{p_0}{\omega_0 v_F^3}} \left[c_\omega \left(\frac{\omega}{\omega_0}\right)^{\frac{2}{3}-2\sigma} + c_q (|q - 2p_F| l_0)^{1-3\sigma} \right] \quad \sigma < 1/3 \quad (24)$$

$$\Pi(\omega, q) = \sqrt{\frac{p_0}{\omega_0 v_F^3}} \left[c_\omega \left(\frac{\omega}{\omega_0}\right)^{2\sigma-\frac{2}{3}} + c_q (|q - 2p_F| l_0)^{3\sigma-1} \right]^{-1} \quad \sigma > 1/3 \quad (25)$$

where the coefficients c_q and c_ω are of the order of unity for a curved Fermi surface. Below we shall assume that $c_q = c_\omega = 1$. Since these coefficients depend strongly on the curvature of the Fermi surface, the case of a flat Fermi surface should be considered separately. We do not discuss it further here.

The spin polarization bubble (25) is equal to the spin susceptibility if the effects of the short range interaction on the spin correlators at $2p_F$ can be neglected. We justify this by showing that a sufficiently weak bare interaction is renormalized to zero by the gauge field. Renormalization of the effective interaction by the gauge field occurs in the two competing channels shown in Fig. 7. In both channels the corrections diverge logarithmically if all external momenta are on the Fermi surface, external energies are zero and the momentum transfer is exactly $Q = 2p_F$. This divergence is again cut off by the largest among ϵ , ϵ_{\parallel} and ϵ_{\perp} . If, say, the largest is the external frequency we evaluate the diagrams in Fig. 7 and get

$$\delta W(\omega) = -2\left(\frac{2}{3} - \frac{1}{2N}\right) \ln\left(\frac{1}{\omega}\right) W_0 \quad (26)$$

where W_0 is the bare interaction at small scales or large frequencies. Using the renormalization group to sum higher orders we conclude that interaction at $2p_F$ decays rapidly at large scales:

anomalous behaviour of the spin correlators at $Q = 2p_F$. In the absence of a short range interaction effective at $2p_F$ (i.e. if the interaction W in eq. 1 vanishes) the spin correlator is given by the polarization diagrams shown in Fig. 6. The leading contributions in powers of $(\frac{1}{N} \ln \omega)$ come from the diagrams in which the vertical lines of the gauge field do not cross. In these diagrams the leading contribution originates from the frequency range (and corresponding momentum range, which we have not explicitly written)

$$\epsilon_F > \omega_n > \dots \omega_1 > \omega < \dots < \omega_{-n} < \epsilon_F$$

where ω is external frequency. Therefore, the sum of all diagrams is given by the diagram shown in Fig. 6 with renormalized vertices (21):

$$W \sim \left(\frac{\omega}{\omega_0}\right)^{\frac{4}{3}-\frac{1}{N}} W_0 \quad (27)$$

Certainly, Eq. (27) holds only for sufficiently small bare interaction W_0 . The decay of the interaction implies that the spin susceptibility $\chi(\omega, q) = \Pi(\omega, q)$. For larger bare interaction $W_0 \geq W_c$ we expect a transition into an ordered state to occur. We will give the theory of this transition in a separate paper. Here we note that at W_c the interaction does not scale and that the basic ingredients of the theory of the transition are polarizability of the fermion system (24,25) and the four spin fluctuation interaction shown in Fig. 8. The renormalization of the four spin interaction may be treated in the same way as that of Π . We find that at large N the leading diagrams are those shown in Fig. 8; these lead to a divergent U with the divergence cut off by the largest among $|\omega/\epsilon_F|^{2/3}$, q_{\parallel}/p_F and q_{\perp}/p_F :

$$U(\omega_1, \omega_2, q_1, q_2) = \frac{\epsilon_F p_F^2}{\left(\frac{\omega}{\epsilon_F}\right)^{4\sigma + \frac{2}{3}} + \left(\frac{|q_\perp|}{p_F}\right)^{12\sigma + 2} + \left(\frac{q_\parallel}{p_F}\right)^{6\sigma + 1}} \quad (28)$$

Here we denote $q_\parallel = \max(|q_1| - 2p_F, |q_2| - 2p_F)$, $\omega = \max(|\omega_1|, |\omega_2|)$ and $q_\perp = (\mathbf{q}_1 - \mathbf{q}_2)\hat{\mathbf{q}}$ where $\hat{\mathbf{q}}$ is the unit vector in the direction of $\mathbf{q}_1 + \mathbf{q}_2$.

To summarize: in the limit of large N the physical properties of the spin liquid resemble conventional Fermi liquid with the following important differences: (i) the scaling relation between energy and momentum is changed to (18), (ii) spin correlators acquire anomalous power behavior (24) at $2p_F$, (iii) interaction vertices with external field at momentum $2p_F$ are strongly enhanced, but (iv) the short ranged interaction between quasiparticles is suppressed.

III. SMALL N LIMIT

In this Section we shall show that in the limit $N \rightarrow 0$ the motion of fermions becomes essentially one dimensional and apply methods borrowed from 1D theories to obtain physical results which turn out to be qualitatively similar to the results obtained in the limit $N \rightarrow \infty$. For the fermion propagator the $N \rightarrow 0$ limit is not singular and the 1D theory gives qualitatively the same result as the $N \gg 1$ 2D calculation. We find that for the vertex function the $N \rightarrow 0$ limit is singular because it predicts an exponentially divergent vertex function rather than the power law derived in the limit $N \rightarrow \infty$. We shall show that the power law behavior remains valid for all finite N , but the power tends to infinity as $N \rightarrow 0$.

The $N \rightarrow 0$ limit is defined via equation (2) for $D(\omega, k)$. In this formula we take N to zero with g^2 constant. To see why this $N \rightarrow 0$ limit is essentially one dimensional consider again the second order (in the gauge field propagator) contribution to the fermion self energy shown in Fig. 2c. Let us perform the integration over k_\perp first. In the limit $N \rightarrow 0$ the k_\perp dependence of the diagram is controlled by the gauge propagators, which

implies that the main contribution is at $k_\perp \sim N^{1/2}\epsilon^{1/3}$; this means that $k_\perp^2 \sim N\epsilon^{2/3}$ is negligible compared to the self energy of the fermion ($\Sigma \sim \epsilon^{2/3}$). Therefore, at $N \rightarrow 0$ one may neglect the k_\perp dependence of all Green function lines. In addition we may neglect all diagrams except those in which all gauge field lines connect two electrons moving either nearly parallel or nearly antiparallel. The reason is that if the gauge field couples two fermions moving in arbitrary directions all components of the transferred momentum are limited by fermion Green functions and become small: $v_F|k| \sim \omega_0^{1/3}|\epsilon|^{2/3}$. This decreases the phase space volume to $k_\parallel k_\perp \sim \epsilon^{4/3}$ (instead of ϵ) and decreases the gauge field propagator to $\sim \epsilon^{-1/3}$. As a result these processes are small (of relative order $\epsilon^{2/3}$) and irrelevant in the infrared limit.

Very similar arguments apply to diagrams containing internal fermion loops other than those contributing to the gauge field propagator. Here the reason is that the gauge field propagator is small in $N^{1/2}$. In the calculation of the fermion propagator this smallness was compensated by the infrared divergence of the integral over momentum component perpendicular to the Fermi velocity. This divergence was cut off by $k_\perp \sim N^{1/2}\omega^{1/3}$ cancelling the factor of $N^{1/2}$. In the diagrams containing fermion loops, momenta in different loops are not exactly parallel ($k_\perp \sim \epsilon^{1/3}$) and integrals over k_\perp are cut off at $k_\perp \sim \epsilon^{1/3}$; this infra-red cut off does not contain compensating factors of N .

In the remaining diagrams one may integrate the gauge field lines over the components of momentum perpendicular to the Fermi velocity and obtain a one dimensional theory of electrons (with propagator depending on frequency and one component of momentum) coupled to the momentum independent but retarded interaction $D^{1D}(\omega)$ defined in (7). As we shall show below, the resulting theory can be solved by bosonization methods. We shall then use Ward identities to obtain information about the behavior at small but non-zero N .

Therefore, in the limit $N \rightarrow 0$ the sum of all diagrams can be found from a mapping to a 1D theory¹¹ with the action

$$S = \int \left(\bar{\Psi}_{-\omega, -k}^{R,a}(i\omega - v_F k) \Psi_{\omega, k}^{R,a} + \bar{\Psi}_{-\omega, -k}^{L,a}(i\omega + v_F k) \Psi_{\omega, k}^{L,a} + \frac{v_F g |\rho_{\omega, k}^R - \rho_{\omega, k}^L|^2}{|\omega|^{1/3}} \right) (dk d\omega) \quad (29)$$

Here $\rho_{t,x} = \bar{\Psi}_{t,x}^a \Psi_{t,x}^a$ is the density operator and a is a replica index which runs over K values. We take the limit $K \rightarrow 0$ to exclude fermion loops, which we have argued to be negligible. In a conventional one dimensional theory with short range interactions loops would be present and would affect the values of the exponents. Our $N \rightarrow 0$ limit is defined so that loops are negligible in the $d = 2$ gauge problem. If loops are *not* negligible in the $d = 2$ gauge problem, their effect is *not* correctly given by the 1D theory.

To compute the fermion propagator we may restrict our attention to the right moving particles. The theory is then the Tomonaga model with a retarded interaction, and has been solved by bosonization¹¹ yielding

$$G(\mathbf{p}, \epsilon) = \int G(x, t) e^{i\epsilon t - i(|\mathbf{p}| - p_F)x} dt dx,$$

$$G(x, t) = \frac{i}{2\pi(x - iv_F t)} \exp\left(\frac{-\Gamma(2/3)l_0^{-1/3}|x|}{(|x| - i\text{sgn}(x)v_F t)^{2/3}}\right),$$

In the limit of low energy and momenta close to the Fermi surface $G(\mathbf{p}, \epsilon)$ acquires a simpler scaling form

$$G^{(1D)}(\epsilon, p) = \frac{-1}{v_F(p - p_F)} g \left(\frac{\Gamma(2/3) l_0^{-1/3} \epsilon^{2/3}}{v_F^{2/3} (p - p_F)} \right) \quad (30)$$

$$g(u) = \frac{3}{2} \exp[(-1)^{3/4} u^{3/2}] - \frac{3\sqrt{3}i}{4\pi} \int_0^\infty \frac{\exp[-(uy)^{3/2}] dy}{y^2 + iy - 1}$$

Although the Green functions (30) and (9) have completely different analytical structures their qualitative properties are similar: both are equal to $1/v_F|p_F - p|$ in the limit $\omega_0^{1/3}|\epsilon|^{2/3} \ll v|p - p_F|$ and both behave as $1/(\omega_0^{1/3}|\epsilon|^{2/3})$ in the opposite limit $\omega_0^{1/3}|\epsilon|^{2/3} \gg v|p - p_F|$. We therefore expect a smooth crossover from formula (30) to (9) as $N \rightarrow 0$. Both describe overdamped fermions with a characteristic energy that scales as $(p - p_F)^{3/2}$. Thus, the limit $N \rightarrow 0$ is not singular for the fermion Green function. Khveschenko and Stamp¹⁴ obtained via eikonal methods a form very similar to (30). They claimed their result was asymptotically exact for all N . Our derivation, on the other hand, suggests that the precise form depends on two special “one-dimensional” features: the neglect of internal loops and the neglect of the perpendicular momentum in fermion propagators. Both these features are present in the $N \rightarrow 0$ limit and in eikonal approximation of Khveschenko and Stamp, but are not present at arbitrary N . Of these two approximations the most crucial is the neglect of the perpendicular momentum. If the p_\perp dependence of the bare Green functions is retained the dressed Green function will not have the exponential form (30). We do not give the algebra here but below we apply similar arguments to the $2p_F$ vertex. If the p_\perp dependence is neglected but loops are taken into account, the one dimensional formalism will lead to Eq. (30) but with a renormalized argument. For this reason we do not believe that the exponential form is generic, although the correspondence between the $N \rightarrow 0$ and $N \rightarrow \infty$ limits lead us to believe that the scaling $\epsilon^{2/3} \propto p_\parallel$ is. Kwon et al¹² also obtained a result

$$\Gamma_{\epsilon, p}^{(1D)}(\omega, q) = \frac{G^{-1}(\epsilon + \omega/2, p + q/2) - G^{-1}(\epsilon - \omega/2, p - q/2)}{i\omega - vq} \quad (33)$$

This identity implies that the singular part of the product of the full Green function and the renormalized vertex is equal to the singular part of the product of the bare Green function and the bare vertex.

This cancellation no longer holds in two dimensions. Instead in 2D the Ward identity is

$$i\omega\Gamma_{\epsilon, p}^0(\omega, q) - q_\parallel\Gamma_{\epsilon, p}^\parallel(\omega, q) - q_\perp\Gamma_{\epsilon, p}^\perp(\omega, q) = G^{-1}(\epsilon + \omega/2, p + q/2) - G^{-1}(\epsilon - \omega/2, p - q/2) \quad (34)$$

Here we have distinguished the density vertex Γ^0 from the two components of the current vertex, and we have written the two components of the current vertex in coordinates parallel and perpendicular to $\mathbf{v}_F(\mathbf{p})$. The gauge field couples to fermions via the current vertex.

In the one dimensional Tomonaga model Γ^\perp is absent and $\Gamma^\parallel = v_F\Gamma^0 = v_F\Gamma^{1D}$ because the current is proportional to the density for fermions moving in one direction. In a general two dimensional theory Γ^0 , Γ^\parallel and Γ^\perp are not simply related; however, in the present model which has only small angle scattering the identity $\Gamma^\parallel = v_F\Gamma^0$ is still valid up to terms of the order of $\epsilon^{2/3}$ or q_\perp^2 . Further, we show in Appendix A that at sufficiently small q_\perp , Γ^\parallel and Γ^\perp are related via:

very similar to (30) from a two dimensional bosonisation method in the problem of half-filled Landau level. Again, we do not believe the result is correct for any $N > 0$.

We now consider the renormalization of the $2p_F$ vertex. In the strictly 1D limit $N \rightarrow 0$ all diagrams leading to this renormalization coincide with the diagrams of 1D Luttinger model (29) which has both right and left movers. The Luttinger model can be solved by bosonization. One finds¹¹ that the renormalized vertex $\gamma_{2p_F}^R$ grows exponentially:

$$\Gamma_{2p_F}^R(\omega) \sim \exp\left(\frac{3g}{2\pi|\omega|^{1/3}}\right) \quad (31)$$

In order to understand the reason for such rapid growth it is convenient to consider the calculation diagrammatically. In order to obtain the renormalization of the $2p_F$ vertex in a conventional Luttinger liquid with a short range interaction v_{SR} one first notices that the first correction to the $2p_F$ vertex is logarithmic; then it can be proved that renormalization of v_{SR} cancels with the fermion self energy²⁰, so that the leading contribution to the $2p_F$ vertex comes from the ladder sum. In each block of this ladder one can use bare vertices and Green functions; finally, the ladder sum exponentiates leading to a power law dependence with exponent determined by v_{SR} . In the present problem the singular interaction means that the first correction, $\delta\Gamma_{2p_F}$, to the bare $2p_F$ vertex $\Gamma_{2p_F}^0$ is a power law,

$$\delta\Gamma_{2p_F} = \Gamma_{2p_F}^0 \frac{3g}{2\pi|\omega|^{1/3}} \quad (32)$$

but renormalization of the interaction $\frac{3g}{2\pi|\omega|^{1/3}}$ still cancels with the fermion self energy and the series exponentiates leading to the exponential dependence given in (31). The cancellation of the interaction renormalization with the fermion self energy is guaranteed by the Ward identity of the 1D theory. This relates the exact density vertex $\Gamma_{\epsilon, p}^{(1D)}(\omega, q)$ to the exact Green function G , and reads²⁰:

$$\Gamma^\perp(\omega, q) = B(\omega, q) \text{sgn}(q_\perp) \Gamma^\parallel(\omega, q) \quad (35)$$

$$B(\omega, q) = \frac{v_F q_\parallel}{2|q_\perp|} \left(\sqrt{1 - \frac{2\alpha|\omega||q_\perp|}{(v_F q_\parallel)^2}} + i0 - 1 \right) \quad (36)$$

where $\alpha = \frac{N^{1/2} v^2 q^2}{2\pi p_0}$. The range of q over which this result applies is given in Appendix A.

Using (35) and (36) in Ward identity (34) we find

$$\Gamma_{\epsilon, p}^{(0)}(\omega, q) = \frac{G^{-1}(\epsilon + \omega/2, p + q/2) - G^{-1}(\epsilon - \omega/2, p - q/2)}{i\omega - v_F q_\parallel - v_F |q_\perp| B(q_\parallel, \omega)} \quad (37)$$

The vertex of the two dimensional theory differs from the one dimensional vertex (33) by the term proportional to q_\perp in the denominator of (37). Although this term is small in the limit $N \rightarrow 0$, it is important because it smears the singularity which appears at $\omega = v_F q_\parallel$ in the 1D theory. From (37) we can calculate the renormalization of the $2p_F$ vertex as was done for the strictly 1D theory. Consider the diagram shown in Fig. 5a, put the external Green functions on the mass shell and use (37). The result is

$$\delta\Gamma_{2p_F} = \int dk_\parallel dk_\perp d\omega \frac{1}{|i\omega - v k_\parallel - |k_\perp| B(\omega, k_\parallel)|^2} \frac{1}{\frac{N p_0 |\omega|}{2\pi |k_\perp|} + \frac{1}{N^{1/2} g^2} |k_\perp|^2} \quad (38)$$

The k integral in (38) is dominated by $k \sim k_\omega \propto |\omega|^{1/3}$; for k_\perp in this range we estimate $B(\omega, k_\parallel) \sim \frac{\omega}{v_F k}$ which implies that the k_\parallel integral is dominated by the region $k_\parallel \sim \sqrt{\frac{\omega k_\perp}{v_F}} \ll k_\omega$ while the main contribution to the k_\perp integral comes from the region $k_\perp \sim k_\omega$. Combining these estimates with Eq. (5) gives

$$\begin{aligned} \delta\Gamma_{2p_F} &\sim \frac{1}{N} \int \frac{d\omega dk_\perp}{(\omega k_\perp)^{1/2}} \frac{k_\perp}{\omega [1 + (k_\perp/k_\omega)^3]} \\ &\sim \frac{1}{N} \int \frac{d\omega}{|\omega|} \left(\frac{k_\omega}{|\omega|^{1/3}} \right)^{3/2} \sim \frac{1}{\sqrt{N}} \ln \Omega \end{aligned} \quad (39)$$

For a more precise calculation, including the coefficient of $1/\sqrt{N}$, see appendix C. These corrections exponentiate as before leading to a power law form for Γ_{2p_F} with an exponent σ which diverges as $N \rightarrow 0$. Explicitly, we find:

$$\sigma = \frac{16\sqrt{2}}{9\pi\sqrt{N}} + O(1) \quad (40)$$

It is interesting to numerically evaluate the exponent at $N = 2$. We find $\sigma = 0.56$.

From the result for Γ_{2p_F} we may obtain as before an expression for the polarization bubble if the short range $2p_F$ interaction W can be neglected. The calculation of W is similar to that leading to Eq. (27) in the previous section. One obtains a scaling equation

$$\delta W(\omega) = \beta(N) \ln \left(\frac{1}{\omega} \right) W + O(W^2) \quad (41)$$

In a strictly 1D theory, $\beta = 0$ and the leading term in the scaling equation is proportional to W^2 . In our case we find for small N

$$\beta(N) = -|c|\sqrt{N} \quad (42)$$

Because the β function is negative both at small and at large N we believe it is negative at any N . Therefore we may again apply the calculation which lead us to Eq. (24) for polarization bubble, however, since σ diverges as $N \rightarrow 0$, the result is Eq. (25).

IV. HALF-FILLED LANDAU LEVEL

In this section we treat the singular interaction argued⁵ to be relevant to the problem of the half filled Landau level. The physical problem leads to two new features: a Chern-Simons term coming from a singular gauge transformation which eliminates the explicit dependence on magnetic field and a long range Coulomb interaction (absent in the spin liquid case because spinons have no charge). In previous treatments^{5,6,9} the Coulomb interaction was taken to be long ranged. We note that in many experimental situations the device containing the half filled Landau level may also contain a metallic gate which screens Coulomb interaction on length greater than a screening length κ^{-1} . The resulting gauge field propagator which includes the RPA self energy of fermion loops and takes into account the dielectric constant $\hat{\epsilon}$ of the host semiconductor is

$$\tilde{D}(\omega, k) = \frac{1}{\frac{p_0 |\omega|}{2\pi |k|} + \frac{u k^2}{k + \kappa}} \quad (43)$$

Here $u = \frac{e^2}{8\pi\hat{\epsilon}}$ and the appearance of the $1/(8\pi)$ instead of the conventional 2π may be traced to a $1/(4\pi)$ in the coefficient of the Chern-Simons term⁵.

In this section we treat the case $\kappa = 0$; we expect the results to apply if the momenta of interest k'_ω are

greater than κ . In the other limit, one should use the results of the previous section interpolated to $N = 1$. The momenta k'_ω are those for which two terms in denominator of (43) are comparable. At temperature T , typical frequencies are $\omega = 2\pi T$ and, if $\kappa = 0$, we find that typical momenta $k'_T \sim (8\pi p_0 k_B T \hat{\epsilon}/e^2)^{1/2}$. Using a typical Fermi momentum for $Ga - Al - As$ system $p_0 = (4\pi n)^{1/2} \approx 8 \times 10^5 \text{ cm}^{-1}$ and a typical $\hat{\epsilon} = 13$ we find that the unscreened results apply if

$$\kappa [\text{cm}^{-1}] < 4 \times 10^5 T^{1/2} [K] \quad (44)$$

Thus if at $T = 0.1 \text{ K}$ the screening layer is further than 1000 \AA from the 2d electron gas, the unscreened results apply. If it is much closer, then one should use the results of the previous section interpolated to $N = 1$.

We turn now to computations using \tilde{D} (43) with $\kappa = 0$.

$$\Sigma^{(2)}(\epsilon) = v_F^2 \sum'_{\omega_1, \omega_2} \int \frac{(dk_1)}{\frac{p_0|\omega_1|}{2\pi|k_1|} + u|k_1|} \frac{(dk_2)}{\frac{p_0|\omega_2|}{2\pi|k_2|} + u|k_2|} \frac{A}{A^2 + \frac{v_F}{p_0} k_1 k_2} \quad (46)$$

with

$$A(\omega_1, \omega_2, p_{\parallel}) = v_F p_{\parallel} + \Sigma^{(1)}(\epsilon + \omega_1 + \omega_2) + \Sigma^{(1)}(\epsilon + \omega_1) + \Sigma^{(1)}(\epsilon + \omega_2)$$

The prime on $\sum_{\omega_1, \omega_2}$ denotes the constraint that sum over frequencies is restricted to the region where $\omega_1 + \omega_2 + \epsilon$ has sign opposite to $\omega_1 + \epsilon$ and $\omega_2 + \epsilon$. This constraint implies that ω_1 and ω_2 cannot vanish simultaneously, so no infra-red singularities arise from the frequency integrals. To extract the infra-red behavior of (46) we may replace A by its typical value $\epsilon \ln(\epsilon_F/\epsilon)$ and $\omega_{1,2}$ by their typical values ϵ . The sum over frequency gives a factor of ϵ^2 . The main contribution to the integrals over k_1, k_2 is a logarithmic divergence coming from the region $\epsilon < q^2 < \epsilon \ln \epsilon$; the final result is

$$\Sigma^{(2)}(\epsilon) = \frac{\hat{\epsilon} v_F}{e^2} \epsilon \frac{\ln^2 \ln(\epsilon_F/\epsilon)}{\ln \epsilon_F/\epsilon} \quad (47)$$

This is smaller than the leading term by the factor

$$\left(\frac{\ln \ln(\epsilon_F/\epsilon)}{\ln(\epsilon_F/\epsilon)} \right)^2$$

Similar considerations apply to higher order crossed graphs.

Our result, that the leading behaviour at small frequencies is given exactly by the first order diagram, is reminiscent of the Migdal theorem¹⁵, which states that the leading low-frequency behavior of the electron self-energy in the electron-phonon problem is given exactly by the leading order diagram. The physical fact underlying Migdal theorem is that the momentum transferred in an electron-phonon process is large (of the order of p_F) while the energy is small (of the order of Debye frequency and much less than $v_F k_F$). A very similar argument applies here. In the calculations leading to Eq. (45) the

The leading order self energy (Fig. 2) is

$$\Sigma^{(1)}(\epsilon) = -i \frac{2\hat{\epsilon} v_F}{\pi e^2} \ln \left(\frac{\epsilon_F}{|\epsilon|} \right) \epsilon + \dots \quad (45)$$

Here the ellipsis indicates terms which are less singular as $\epsilon \rightarrow 0$. Arguments identical to those of section II show that $\Sigma^{(1)}$ also solves the leading order Eliashberg equation, so it sums correctly all rainbow graphs.

We now argue that higher order crossed diagrams give less singular contributions to $\Sigma(\epsilon, p)$, so that the leading dependence is given exactly by (45). Consider the leading crossed diagram, Fig. 2c, with the fermion propagators dressed by the self energy (45). After integration over parallel momenta and symmetrization in $q_{\perp 1}, q_{\perp 2}$ one finds

energy transferred by the gauge field is small, while the integral over momenta is logarithmic and only cut off at the scale p_F . In the spin liquid case discussed in the previous Sections all momentum integrals were confined to the region of small momenta. The problem simplified only in the large N limit where the range of the momentum integration became large in N . Thus, the problem of half-filled Landau level is analogous to the large N limit of the spin liquid case. Kwon et al¹² obtained a somewhat different result for the fermion Green function via a two dimensional bosonisation method. Their result is equivalent to applying our previously discussed $N = 0$ bosonisation technique to the half-filled Landau level problem. As explained in Section III we do not believe this is a correct procedure.

We now turn to polarization bubble and vertices. As in the previously considered spin liquid case, the only singularities occur in the $2p_F$ vertices. The leading $2p_F$ vertex correction, Fig. 5a, is given after summing over parallel momenta by

$$\Gamma_{2p_F}^{(1)} = v_F \sum_{\epsilon} \int \frac{(dk)}{\frac{p_0|\epsilon|}{2\pi|k|} + \frac{\epsilon^2}{8\pi\hat{\epsilon}}|k|} \frac{1}{\frac{2\hat{\epsilon} v_F}{\pi e^2} |\epsilon| \ln \epsilon + \frac{v_F}{p_0} k^2} \quad (48)$$

Again, the leading contribution to the integral over k_{\perp} is a logarithm coming from the region $\epsilon < v_F k_{\perp}^2/p_0 < \epsilon \ln \epsilon$. Performing this integral and evaluating the sum over frequencies we get

$$\Gamma_{2p_F}^{(1)} = \frac{1}{2} \ln^2 \left[\ln \left(\frac{\epsilon_F}{\max(T, \omega, v_F(Q - 2p_F)^2/p_0)} \right) \right] \quad (49)$$

Although it is of only academic interest, we note that the higher order corrections may be summed to obtain the leading singular behavior. As in the case of the self-energy, crossed graphs are less singular than ladder ones. As in Section II, the sum of the ladder graphs exponentiates, leading to

$$\Gamma_{2p_F} = \exp \left[\frac{1}{2} \ln^2 \left[\ln \left(\frac{\epsilon_F}{T} \right) \right] \right] \quad (50)$$

This weak singularity implies that the polarizability is not singular, but the leading frequency and momentum

$$\begin{aligned} S_{eff} = & \int (d\omega d^d k) \Psi_{\omega, k}^\dagger [|\omega|^{d/(2+x)} - v_F k_{\parallel} + \frac{v_F}{2p_0} k_{\perp}^2] \Psi_{\omega, k} + \int (d\omega d^d q) (|q|^{1+x} + \frac{p_0 |\omega|}{|q|}) |a(\omega, q)|^2 \\ & + g \int (d\omega_1 d^d k_1) (d\omega_2 d^d k_2) \Psi_{\omega_1, k_1}^\dagger \Psi_{\omega_2, k_2} [\mathbf{v}_F(k_1) + \mathbf{v}_F(k_2)] (\mathbf{a}(\omega_1 - \omega_2, k_1 - k_2) + h.c) \end{aligned} \quad (51)$$

We find that the fermion-gauge-field interaction g is irrelevant for $d > 2$ and marginal in $d = 2$. Further, for $x > 0$ in $d = 2$ the marginality of the interaction leads to logarithms only in the $2p_F$ response functions.

Note that S_{eff} involves dressed fermions with one-loop self-energy $\Sigma = |\omega|^{d/(2+x)}$ rather than the linear ω dependence expected for unrenormalized fermions. As shown by Nayak and Wilczek⁹, if the linear ω dependence is used in S_{eff} , then the fermion-gauge-field interaction g is relevant for $d < 2 + x$, and is in particular relevant in $d = 2$ for $x > 0$. We argue that the strong-coupling fixed point to which the Nayak-Wilczek scaling flows is simply the S_{eff} we have written above. The argument has two steps. The first is the known result¹⁰ that the first order correction to the fermion propagator from the gauge field interaction is of the form $|\omega|^{d/(2+x)}$. The second step is that further corrections do not change the form given by the first order correction. We have shown this in previous sections by explicit solutions of the model in two limits. In this section we give a scaling argument leading to the same conclusion.

We first explain our choice of notation in more detail; it comes from the fact, seen in the calculations of the previous sections, that a gauge fluctuation of momentum \mathbf{q} couples primarily to fermions in a patch of the fermi surface where the fermion velocity \mathbf{v}_F is perpendicular to the direction of \mathbf{q} . Therefore, in the effective action we have written the momentum dependence of the fermion fields using local coordinates defined in a patch centered on the point (in $d = 2$) or strip (in $d = 3$) of the fermi surface where \mathbf{v}_F is perpendicular to \mathbf{q} . In this patch the gauge-field-fermion interaction is simplified because the transverse component of the gauge field is almost parallel to \mathbf{v}_F , so we may replace the cosine of the angle between the gauge field \mathbf{a} and \mathbf{v}_F by unity.

To see that this construction is reasonable, note that from the gauge field propagator in S_{eff} we learn that at frequency ω the important momentum scale is $|\omega|^{1/(2+x)}$. From the fermion propagator we learn that the impor-

dependence is weakly singular.

V. SCALING

In this section we recover some of the results obtained in previous sections via a scaling analysis. Our principal result concerns the properties of the effective action S_{eff} of dressed fermions, Ψ , coupled to a gauge field \mathbf{a} in d spatial dimensions:

tant momentum scale in the direction perpendicular to the fermi surface is $|\omega|^{d/(2+x)}$; for $d > 1$ this is always much less than the scale defined from the gauge propagator, so that the momentum transferred from the gauge field to the fermion is essentially perpendicular to the fermi velocity, and the patch construction is well defined. Also from the fermion propagator we see that the k_{\perp} scale is $|\omega|^{\frac{d}{2(2+x)}}$. Thus in $d > 2$ the dependence of the fermion propagator on k_{\perp} is essential. In $d = 2$, the momentum scale derived from the gauge field and from the fermion propagator are the same, and the importance of the curvature term $k_{\perp}^2/(2p_0)$ is determined by a dimensionless parameter (e.g. N). We see that in these arguments the curvature of the Fermi surface (specified by p_0^{-1}) is essential. We shall show below that p_0^{-1} changes under scaling, so one must interpret it as a charge in the renormalization group equations.

We now discuss the ‘‘tree-level’’ scaling procedure. The theory has three coordinates: frequency, k_{\parallel} , and q (which we have shown is the same as k_{\perp}). All three scale differently. We choose the scaling of k_{\parallel} following Shankar¹⁶: that is, we imagine integrating out fermions in a shell given by $\Lambda/b < \epsilon_k < \Lambda$ about the Fermi surface and then rescaling the momentum perpendicular to the fermi surface to restore the upper cut off. We then choose the scaling of frequency to keep the $|\omega|^{d/(2+x)}$ term in the fermion action invariant, and then choose the scaling of q (which is the same as that of k_{\perp}) to keep the gauge field propagator invariant. Finally, we choose the scaling of the fields to compensate for the scaling of the coordinates and integrals, so that the quadratic terms remain invariant. Note that we must interpret $\int d^d q$ in the gauge field term or the fermion field term as $\int dq_{\parallel} d^{d-1} q_{\perp}$. This implies

$$\Psi \rightarrow \Psi b^{\frac{3d+1+x}{2d}}$$

$$a \rightarrow ab^{\frac{d+1+x}{d}}$$

Combining all factors we get the following tree-level scaling equations for the charges $1/p_0$ and g :

$$\begin{aligned}\frac{dp_0^{-1}}{d \ln b} &= \left(1 - \frac{2}{d}\right) p_0^{-1} \\ \frac{dg}{d \ln b} &= 0\end{aligned}$$

Therefore, the gauge-field fermion coupling is marginal for $d \geq 2$ but in $d > 2$ the effective curvature of the fermi surface grows. For large curvature the usual arguments leading to the Migdal theorem¹⁵ imply that the crossed graphs may be neglected, so we may restrict ourselves to the leading order of perturbation theory, which gives the self energy $|\omega|^{\frac{d}{2+x}}$.

Alternatively, one may consider a scaling procedure which preserves the form of the fermion propagator. In this case one must scale k_{\perp} as $b^{-1/2}$ and in $d > 2$ both the coefficient of the q^{1+x} term in the gauge propagator and gauge-field-fermion coupling g scale to zero (indeed the tree-level scaling equation for g becomes $\frac{dg}{d \ln b} = \frac{2-d}{4}$, so that a manifestly weak coupling fixed point is obtained).

In $d = 2$, however, all charges are marginal for all $x > 0$ and further analysis beyond tree level is needed to determine which physical quantities are renormalized. For our purposes the most efficient method of deriving the one-loop renormalization group equations is to use the technique of differentiating the one-loop diagrams with respect to the upper cut off. The calculations presented in the previous sections can be carried over directly to show that the only quantities which are renormalized are the $2p_F$ vertex Γ_{2p_F} and polarizability $\Pi(2p_F)$. In particular, neither p_0 nor g scales in $d = 2$. Rewriting Eq. (19) in the notations of this section (here we normalize to k_{\parallel} and in the previous section we normalized to frequency) we find

$$\frac{d\Gamma_{2p_F}}{d \ln b} = \frac{2+x}{2} \sigma \Gamma_{2p_F} \quad (52)$$

where σ is a number which depends on the fixed point values of p_0 and g . Our results of the previous sections may be viewed as calculations of the fixed point values of p_0 and g in the large and small N limits.

Although there are no logarithmic corrections to the fermion propagator, the finite renormalizations generated by marginally irrelevant operators do mean that the fermion propagator $G^{-1}(\epsilon, p_{\parallel}, p_{\perp})$ is not precisely given by the form $|\epsilon|^{\frac{2}{2+x}} - v_F(p_{\parallel} + p_{\perp}^2/(2p_0))$ written in Eq. (51) when $|\epsilon|^{\frac{2}{2+x}}$, $v_F p_{\parallel}$ and $p_{\perp}^2/(2p_0)$ are of the same order, although the limits when one argument is much larger than the others are correctly given.

Finally, we consider $d = 2$, $x = 0$. Here at tree level we would conclude that for the action with inverse fermion propagator $(\omega - v_F k_{\parallel} + \frac{v_F}{2p_0} k_{\perp}^2)$ and for inverse gauge propagator $(|q| + \frac{|\omega|}{|q|})$ the fermion-gauge-field coupling is marginal. However, caution should be exercised in deriving renormalization group equations beyond tree level,

because in the two-loop calculations presented in the previous section no terms of order $(\ln \Lambda)^2$ were found so that the logarithms found in one-loop order do not sum to powers. Instead, the calculations presented in section IV show that the asymptotic form of the fermion propagator is $i\omega \ln |\omega| - v_F k_{\parallel} - \frac{v_F}{2p_0} k_{\perp}^2$, and the $2p_F$ vertices are extremely weakly singular ($\sim \exp \frac{1}{2} \ln^2 \ln \omega$).

VI. CONCLUSION

We have presented a discussion of the low energy properties of a system of fermions in spatial dimension d coupled via a singular gauge interaction with propagator $D(\omega, q) = (|\omega|/|q| + |q|^{1+x})^{-1}$. We found that the fermion lifetime scales as $|\omega|^{\frac{d}{2+x}}$ (in $3 \geq d \geq 2$, $x > 0$) and that in $d = 2$ the $2p_F$ fermion polarizability $\Pi(\omega, q)$ was non-analytic and possibly divergent as $Q \rightarrow 2p_F$ and $\omega \rightarrow 0$. Whether or not the susceptibility is divergent depends on the value of an exponent, σ , which we could calculate only in certain unphysical limits. In the spin liquid case $x = 1$ extrapolation of our calculated σ to the physical limit of spin degeneracy $N = 2$ from two sides yielded estimates for σ bracketing the critical value $\sigma_c = 1/3$ above which Π diverges. In the $\nu = 1/2$ case one must distinguish between screened and unscreened Coulomb interactions. In the unscreened case, $x = 0$, the self energy is $\omega \ln \omega$ while the nonanalyticity in the $2p_F$ vertex is very weak: $\exp(\frac{1}{2} \ln^2[\ln|\omega|])$ and the polarizability does not diverge. In the screened case the results for $x = 1$ apply with spin degeneracy $N = 1$ and our estimates suggest that the $2p_F$ polarizability diverges.

There is a simple physical interpretation for the non-analyticities at $2p_F$: a moving fermion emits a gauge field which relaxes so slowly that if at a later time the fermion is scattered backwards it meets the gauge field again and is able to lower its energy. It is remarkable that this physics can lead to an actual divergence of the $2p_F$ susceptibility if the fermion-gauge-field interaction is strong enough. The form of the divergence is given in Eq. (24,25) and is controlled by an exponent σ which can a priori take any value. However, we note that if $\sigma \geq 7/6$, then $\sum_{\omega, q} \Pi(\omega, q)$ is infrared divergent. Such a divergence is not possible; for example in a magnetic system this would imply that the expectation value of the square of the local spin density $\langle S_i^2 \rangle$ diverges. Therefore we believe that for $\sigma \geq 7/6$ some other physics beyond the scope of our calculations must intervene to cut off the divergence. One mechanism for this feedback can be seen in the spin-fluctuation contribution to the electron self-energy. For $\sigma \geq 7/6$ this diverges, implying a smearing of the Fermi surface which would suppress the Fermi surface singularities we have found. However, for $7/6 > \sigma > 1/3$ we believe this critical phase is stable.

In order to understand the physical properties of the critical phase, consider first a translation-invariant electron gas (as is realized in the half-filled Landau level).

Then Eq. (25) would predict that the susceptibility diverges as $T \rightarrow 0$ on a ring of radius $2p_F$. For fermions on a lattice, the situation is more complicated for reasons very similar to those analysed by Littlewood et al²¹ in a study of $2p_F$ singularities in a marginal Fermi liquid picture. First, instead of a circle of radius $2p_F$ one obtains one or more curves traced out by the vectors \mathbf{Q} connecting points with parallel tangents. Second, the amplitude (but not the exponent) of the divergent term in χ_{2p_F} varies around the curve due to the variation of v_F and p_0 around the Fermi surface. Third, one obtains additional families of curves on which χ diverges. These are generated by $\mathbf{Q} + \mathbf{G}$ where \mathbf{G} is any vector of the reciprocal lattice. As a result one gets additional peaking when members of different families intersect. The result, for band structures appropriate to high- T_c superconductors will be a susceptibility strongly peaked at particular points in q -space which might be qualitatively consistent with neutron data for $La_{2-x}Sr_xCuO_4$ ²¹. In addition, the divergent spin fluctuations imply that the Cu NMR rate $1/T_1T \propto 1/T^{2\sigma-1/3}$, so the $1/T_1T$ diverges as $T \rightarrow 0$ even at the borderline value $\sigma = 1/3$. The value $\sigma = 2/3$ would lead to $1/T_1T \propto 1/T$ consistent with Cu NMR experiment on high- T_c superconductors. Of course, if these

wavevectors where $\chi''(\omega, q)$ is maximal are too far from the commensurate wavevector (π, π) , the oxygen $1/T_1T$ will also diverge, in disagreement with experiment²².

In the half-filled Landau level case with screened Coulomb interaction the divergence in the $2p_F$ susceptibility could in principle be observed in sound propagation experiments in which the phonon wavevector is tuned to $2p_F$. The divergence should lead to a large damping of the phonon which increases as T is decreased. The effect should be observable for temperatures and phonon frequencies less than a scale ω_0 which we calculate from Eqs. (3,4,43). We rewrite the expression for ω_0 in terms of the Fermi energy $\epsilon_F = \hbar^2 p_F^2 / (2m)$, Coulomb parameter $E_c = \frac{e^2 n^{1/2}}{\epsilon}$ and the screening length κ^{-1} , obtaining

$$\hbar\omega_0 \approx 0.15 \frac{\epsilon_F^3 \kappa^2}{n E_c^2} \quad (53)$$

Assuming typical numbers for $GaAlAs$ inversion layers $m = 0.07m_e$, $\epsilon = 13$ and $n = 10^{11} \text{ cm}^{-2}$ we have $E_F \sim 50 \text{ K}$ and $E_c \sim 40 \text{ K}$ so $\hbar\omega_0 [\text{K}] \approx 10 \frac{\kappa^2}{n}$. Thus if the screening length is not too much greater than the interparticle spacing, the effect should be observable.

APPENDIX A: VERTEX AT LOW MOMENTUM TRANSFER

Here we use the Ward identity to derive the exact form of the renormalized fermion-gauge-field vertex at low momentum transfer q_\perp and q_\parallel (the exact conditions under which this form applies will be obtained below). In this

$$i\omega\Gamma_{\epsilon,p}^0(\omega, q) - q_\parallel\Gamma_{\epsilon,p}^\parallel(\omega, q) - q_\perp\Gamma_{\epsilon,p}^\perp(\omega, q) = G^{-1}(\epsilon + \omega/2, p + q/2) - G^{-1}(\epsilon - \omega/2, p - q/2)$$

Here Γ^0 is the density vertex and Γ^\parallel and Γ^\perp are the components of the current vertex parallel and perpendicular to $\mathbf{v}_F(\mathbf{p})$. We wish to obtain from this an equation relating Γ^0 to the fermion Green function. As noted previously, in the present model at small q, ω the current vertex Γ^\parallel is related to the density vertex Γ^0 by $\Gamma^\parallel = v_F\Gamma^0$. We now derive the relation between Γ^\perp and Γ^0 . Consider a high order diagram for Γ^\perp of the type shown in Fig. 9a, in which *one* of the gauge field lines connecting one external fermion leg to the other is isolated, i.e. not crossed by any other gauge field line connecting one external fermion leg to another. The analytical expression has the general form

$$\Delta\Gamma^\perp = \frac{v_F}{p_0} \int \prod_j (d^2k_j) \sum_{i=1}^{i=n} k_{\perp i} \prod_j D(k_j) \prod G \quad (A1)$$

where index i runs over n values corresponding to the gauge field lines connecting different legs and we did not

limit the renormalized vertex becomes singular, and our goal is to find the form of this singularity. The expression that we shall find is correct at any N for sufficiently small transferred momenta q_\perp, q_\parallel . The value of N determines only the range of q_\perp, q_\parallel over which the expression obtained in the limit of very low momenta remains valid.

The fundamental Ward identity was given in Eq. (34); we repeat it here for convenience.

explicitly write the arguments of the fermion Green functions G . Label the momentum of an "uncrossed" gauge field line by \mathbf{k}_a , and pick out the term in the sum proportional to $k_{\perp a}$. We show below that all other terms in the sum are small.

In the limit $q_\perp \rightarrow 0$ the fermion Green functions in diagrams such as Fig. 9a depend only on the combination $(k_{\parallel a} + k_{\perp a}^2/2p_0)$, so their dependence on $k_{\perp a}$ can be completely eliminated by the shift $k_\parallel \rightarrow k_\parallel - k_\perp^2/2p_0$. (Recall that the k_\parallel dependence of D is negligible always). After this transformation the only remaining dependence on $k_{\perp a}$ is in $D(k_{\perp a})$. The remaining integration over k_\perp is straightforward:

$$\int D(k_{\perp a}) k_{\perp a} dk_{\perp a} = 0 \quad (A2)$$

This integral converges poorly at large k_\perp , because the integrand decreases as $\sim 1/k_\perp$ at large k_\perp , but is zero at $q_\perp = 0$, because the integrand is an odd function of

k_{\perp} . At any $q_{\perp} \neq 0$ the dependence of the Green functions on the momentum k_{\perp} can no longer be neglected. Since Green functions depend only on the product $q_{\perp} k_{\perp}$, their k_{\perp} dependence becomes significant only at large $k_{\perp} \sim \Sigma(\epsilon)/q_{\perp}$. At smaller k_{\perp} the dependence of the Green function on k_{\perp} can be neglected and the contributions from positive and negative k_{\perp} cancel each other. Because the main contribution to this diagram comes from large $k_{\perp a} \sim \Sigma(\epsilon)/q_{\perp}$, the Migdal arguments of Sections II and III show that at large k_{\perp} all diagrams in which other lines cross the line with large momentum transfer are small.

Now consider any arbitrary diagram for Γ^{\perp} . The corresponding analytical expression will be of the form shown in eq. (A1). Pick out one term in the $\sum_{i=1}^{i=n} k_{\perp i}$. The di-

$$\Gamma_{\epsilon, \mathbf{p}}^{\perp}(\Omega, \mathbf{q}) = \frac{N^{1/2} g^2 v_F^3}{p_0} \Gamma_{\epsilon, \mathbf{p}}^0(\Omega, \mathbf{q}) \quad (\text{A3})$$

$$\times \int \Gamma_{\epsilon+\omega, \mathbf{p}+\mathbf{k}}^0(\Omega, \mathbf{q}) G(\epsilon+\omega+\Omega/2, p+k+q/2) G(\epsilon+\omega-\Omega/2, p+k-q/2) \frac{(d^2 k d\omega)}{k_{\perp}}$$

In this equation the vector character of the vertex is expressed via the factor of k_{\perp}^{-1} which may be positive or negative. Together with Ward identity Eq. (34), Eq. (A3) forms a closed system of equations for the vertex Γ^0 . To solve it we introduce the notation

$$\Gamma_{\epsilon, \mathbf{p}}^{\perp}(\omega, \mathbf{q}) = v_F B(q_{\parallel}, q_{\perp}) \Gamma_{\epsilon, \mathbf{p}}^0(\omega, \mathbf{q}) \quad (\text{A4})$$

Here we have suppressed the dependence of B on the frequency ω , because ω is a dummy variable in the analysis that follows. We use the Ward identity to express Γ^0 in Eq. (A3) through $B(q_{\parallel}, q_{\perp})$, finding:

$$B(q_{\parallel}, q_{\perp}) = \frac{v_F g^2 N^{1/2}}{p_0} \int \frac{(d^2 k d\omega)}{k_{\perp}} \frac{G(\epsilon+\omega+\Omega/2, p+k+q/2) - G(\epsilon+\omega-\Omega/2, p+k-q/2)}{i\Omega - v_F(q_{\parallel} + \frac{q_{\perp} k_{\perp}}{p_0}) - q_{\perp} v_F B(q + \frac{q_{\perp} k_{\perp}}{p_0}, q_{\perp})} \quad (\text{A5})$$

Integrating over k_{\parallel} and ω and scaling the k_{\perp} variable ($k_{\perp} \rightarrow k_{\perp} p_0/q_{\perp}$) we find:

$$B(q_{\parallel}, q_{\perp}) = \alpha \operatorname{sgn} q_{\perp} P \int \frac{dk}{2\pi k} \frac{i\tilde{\Omega}}{i\tilde{\Omega} - (q_{\parallel} + k) - B(q_{\parallel} + k, q_{\perp}) q_{\perp}} \quad (\text{A6})$$

where $\tilde{\Omega} = \Omega/v_F$ and

$$\alpha = \frac{v_F g^2 N^{1/2}}{p_0} \quad (\text{A7})$$

is a dimensionless parameter of the order of $N^{1/2}$. It is convenient to consider positive and negative Ω separately. The considerations are similar so we consider explicitly only $\Omega > 0$ here. Equation (A6) can be simplified if we assume that the denominator in it has poles only in the upper half plane. We shall show this assumption is self-consistent. In this case the integration contour can be closed in the lower half plane and the integral equation simplifies to the algebraic equation

$$B(q_{\parallel}, q_{\perp}) = \frac{1}{2} \frac{\alpha \tilde{\Omega}}{i\tilde{\Omega} - (q_{\parallel}) - q_{\perp} B(q_{\parallel}, q_{\perp})} \quad (\text{A8})$$

Solving it we find

agram will be important only if the gauge field line carrying this momentum is "uncrossed" in the sense discussed above. This justifies the assumption made above that the term in the sum proportional to $k_{\perp a}$ corresponds to an "uncrossed" line. Therefore, the diagrams which give the dominant contribution at small q_{\perp} can be represented as the diagram shown in Fig. 9b. Here the two blocks involve gauge field lines which cross each other and the double wavy line represents $D(k_{\perp a})k_{\perp a}$. Since the integral over k_{\perp} in the double wavy line is dominated by large k_{\perp} , the frequency dependence of it can be neglected while the dependence on k_{\parallel} can be neglected always. For this reason, the outer block is simply with the bare vertex Γ^0 . The inner block can be also expressed in terms of the vertex Γ^0 . After some manipulation we find:

$$B(q_{\parallel}, q_{\perp}) = \frac{i\tilde{\Omega} - v_F q_{\parallel} + \sqrt{(i\tilde{\Omega} - v_F q_{\parallel})^2 - 2\alpha |q_{\perp}| |\tilde{\Omega}|}}{2q_{\perp}} \quad (\text{A9})$$

Restoring the notations of Section III and using $v_F q_{\parallel} \gg \Omega$ we get the equation (36) announced in Section III.

Combining the Ward identity (34) with Eqs. (A4) and (36) we get the final expression for the vertex at low momentum transfer:

$$\Gamma_{\epsilon, \mathbf{p}}^{(0)}(\Omega, \mathbf{q}) = 2 \frac{G(\epsilon+\Omega/2, p+q/2) - G(\epsilon-\Omega/2, p-q/2)}{v_F q_{\parallel} + \sqrt{(v_F q_{\parallel})^2 - 2\alpha |\Omega| |q_{\perp}|} - i\Omega v_F q_{\parallel}} \quad (\text{A10})$$

Thus, Γ^{\perp} is substantially enhanced at low momenta $v_F q_{\parallel} \ll |\omega_0^{1/3}| |\omega|^{2/3}$, $q_{\perp} < (v_F q_{\parallel})^2 / (\alpha |\Omega|)$. This range

of momenta becomes small at $N \gg 1$ because $\alpha \sim N^{1/2}$ and does not contribute much to the self-energy.

The essential ingredient in the derivation of (36) and (A10) was assumption that the momentum k_\perp is sufficiently large so that crossing diagrams can be neglected. We also assumed that $k_\perp \gg k_\omega$ which allowed us to neglect the frequency dependence of the gauge field propagator. Both these conditions are satisfied if $q_\perp \ll \frac{1}{N}k_\Omega$. In the limit $N \gg 1$ this condition limits drastically the range of momentum where (A10) can be applied.

APPENDIX B: HIGHER ORDER DIAGRAMS IN $1/N$

The calculations of Appendix A show that the gauge-field-fermion vertex is enhanced at very low momentum transfer as is evident from Eq. (A10). This equation, however, was derived under the assumption that $q_\perp \ll \frac{1}{N}k_\omega$. At larger momentum transfer q_\perp the corrections to the bare vertex are small, Eq. (A10) is not valid, instead, the leading corrections are given by the first crossing diagram shown in Fig. 3. The straightforward calculation gives Eq. (10). The equation (10) crosses over to the equation (A10) at $q_\perp \sim \frac{1}{N}k_\omega$. So, at

large N the momentum range where the whole series of diagrams should be summed is small in $1/N$, moreover, this momentum range turns out to be so small that it does not contribute even to subleading order in $1/N$ for most quantities. For instance, the contribution of this range to the self energy is of the order of $\frac{1}{N^2}$, whereas the leading term which comes from larger momenta is of the order of $\left(\frac{\ln[N]}{N}\right)^2$ (Eq. (14)). Thus, in order to obtain the subleading terms of the order of $\frac{\ln^2[N]}{N^2}$ it is sufficient to keep only the first crossing diagrams in photon propagator. However, in order to obtain all terms of the order of $\frac{1}{N^2}$ one needs to use the Eq. (A10) and the crossover formulas (which we did not derive) in the range $q_\perp \sim \frac{1}{N}k_\omega$.

Similarly, in the calculation of the exponent of the $2p_F$ vertex, the enhancement of the gauge-field-fermion vertex at $q_\perp \lesssim \frac{1}{N}k_\omega$ leads to corrections of the order of $\frac{1}{N^2}$ to the exponent. As we shall see below, the leading terms are larger by factors of $\ln[N]$, so in the subleading term we again can keep only the simplest crossing diagrams shown in Fig. 5. Only the diagrams shown in Fig. 5b and Fig. 5d have contributions which contain powers of $\ln[N]$. Consider the diagram shown in Fig. 5b. Its analytical expression reads

$$\delta_1\Gamma_{2p_F}(\omega) = v_F^4 \int D(\eta, k)D(\Omega, q)G(\eta, k)G(\Omega + \eta, q + k)G(\Omega, q)G(\Omega + \omega, -q)(d^2q d^2k d\Omega d\eta) \quad (B1)$$

The contribution containing logarithms of N comes from the momentum range $k_\eta > |k_\perp| > |q_\perp| > \frac{1}{\sqrt{N}}k_\Omega$. In this range the self energy parts of the Green functions can be neglected. We integrate over parallel components of momenta k_\parallel and q_\parallel and symmetrize the resulting expression obtaining:

$$\delta_1\Gamma_{2p_F}(\omega) = \frac{p_0^2}{2\pi^4} \int_\omega^\infty d\Omega \int_0^\Omega d\eta \int_0^\infty \frac{dk_\perp dq_\perp}{k_\perp^2 q_\perp^2 - q_\perp^4} \quad (B2)$$

Evaluating the remaining integrals with logarithmic accuracy we get

$$\delta_1\Gamma_{2p_F}(\omega) = \frac{1}{8\pi^2} \frac{\ln^3[N]}{N^2} \ln\left(\frac{1}{\omega}\right) \quad (B3)$$

Evaluation of the diagram shown in Fig. 5d is very similar It has analytical expression

$$\delta_2\Gamma_{2p_F}(\omega) = v_F^4 \int D(\eta, k)D(\Omega, q) \times G(\Omega, k)G(\Omega + \eta, q + k)G(\Omega + \eta + \omega, -(q + k))G(\Omega + \omega, -q)(d^2q d^2k d\Omega d\eta) \quad (B4)$$

We integrate over parallel components of momenta, obtaining after symmetrization:

$$\delta_2\Gamma_{2p_F}(\omega) = \frac{p_0^2}{2\pi^4} \int_\omega^\infty d\Omega \int d\eta \int_0^\infty \frac{\beta|\Omega|^{2/3}|\eta + \Omega|^{2/3} - q_\perp^2(k_\perp + q_\perp)^2 \text{sgn}[\Omega(\Omega + \eta)]}{(\beta|\Omega|^{4/3} + q^4)(\beta|\Omega + \eta|^{4/3} + (q_\perp + k_\perp)^4)} \times D(\Omega, q_\perp)D(\eta, k_\perp)dk_\perp dq_\perp \quad (B5)$$

Here $\beta = 4\left(\frac{p_0}{v_F}\right)^2 \omega_0^{4/3}$. The first term in the numerator of this integral is logarithmically divergent; the main contribution to the integral comes from the frequency

range $\eta > \Omega > \omega$ and results in a $\frac{1}{2N^2} \ln^2(1/\omega)$ contribution which one expects from general renormalization group arguments. The second term in the numerator

has no contribution from this frequency range due to $\text{sgn}[\Omega(\Omega + \eta)]$, so it results in only one power of $\ln(1/\omega)$, instead it contains $\ln[N]$ coming from the momentum range $k_\eta > |k_\perp| > |q_\perp| > \frac{1}{\sqrt{N}}k_\Omega$. In this momentum range we neglect the self energy parts of the Green functions and perform integrals with logarithmic accuracy obtaining:

$$\delta_2\Gamma_{2p_F}(\omega) = \frac{1}{4\pi^2} \frac{\ln^3[N]}{N^2} \ln\left(\frac{1}{\omega}\right) \quad (\text{B6})$$

Adding the contributions from the diagrams in Fig. 5b (which come with a factor of two) and Fig. 5d we get Eq.

$$\delta\Gamma_{2p_F}(\omega) = -v_F^2 \int G(\eta, q)G(\eta + \omega, -q)D(\eta, q)\Gamma_{\eta, q}\left(\frac{\eta}{2}, \frac{q}{2}\right)\Gamma_{-\eta, -q}\left(\frac{\eta}{2}, \frac{q}{2}\right)(d^2q d\eta) \quad (\text{C1})$$

This expression simplifies if the external frequency of the fermion is zero and its momentum is on the Fermi surface because in this case $G^{-1}(\epsilon, p) = 0$ in Eq. (37) for the vertex:

$$\delta\Gamma_{2p_F}(\omega) = \frac{1}{\pi^3} \int_\omega^\infty d\eta \int_0^\infty \frac{4v_F^2 dq_\perp dq_\parallel}{|vq_\parallel + \sqrt{(v_F q_\parallel)^2 - 2\alpha\eta q_\perp}|^2} D(\eta, q_\perp) \quad (\text{C2})$$

Here we replaced the exact dependence on the external frequency ω by an approximate cut off which is sufficient for logarithmic accuracy. Evaluating this integral we get

$$\delta\Gamma_{2p_F}(\omega) = \sigma \ln\left(\frac{1}{\omega}\right) \quad (\text{C3})$$

where σ is given by (40).

APPENDIX C: EXPONENT OF THE $2p_F$ VERTEX IN THE SMALL N LIMIT

In order to find the exponent of the $2p_F$ vertex in the small N limit we evaluate the first correction to the $2p_F$ vertex shown in Fig. 5a using the exact gauge-field-fermion vertices and then exponentiate the result. This prescription is known to work in 1D Luttinger model and it gives the leading terms of the $1/N$ expansion. The analytical expression for Fig. 5a is

¹ L. B. Ioffe and A. I. Larkin, Phys. Rev. **B39**, 8988 (1989).
² G. Baskaran, Z. Zou and P. W. Anderson, Sol. St. Comm. **63**, 973 (1987).
³ P. W. Anderson, Science, **256**, 1526 (1992).
⁴ F. C. Zhang and T. M. Rice, Phys. Rev. B37, 3759 (1988).
⁵ B. Halperin, P. A. Lee and N. Read, Phys. Rev. **B 47**, 7312 (1993)
⁶ V. Kalmeyer and S.-C. Zhang, Phys. Rev. B46, 9889 (1992).
⁷ M. Reizer, Phys. Rev. **40**, 11571 (1989).
⁸ P. A. Lee, p. 96 in **High Temperature Superconductivity: Proceedings**, eds. K. S. Bedell, D. Coffey, D. E. Meltzer, D. Pines, and J. R. Schrieffer, Addison-Wesley (Reading, CA: 1990).
⁹ C. Nayak, F. Wilczek, unpublished.
¹⁰ P. A. Lee, Phys. Rev. Lett. **63**, 680 (1989).
¹¹ L. B. Ioffe, D. Lidsky and B. L. Altshuler (unpublished).
¹² H. J. Kwon, A. Houghton and J. B. Marston (unpublished).
¹³ J. Gan and E. Wong, Phys. Rev. Lett. **71**, 4226 (1993).

¹⁴ D. V. Khveshchenko and P. C. E. Stamp, Phys. Rev. Lett. **71**, 2118 (1993).
¹⁵ A. B. Migdal, Sov. Phys. **J.E.T.P.** **7** 333 (1957) and A. A. Abrikosov, L. P. Gorkov and I. E. Dzyaloshinsky, **Methods of Quantum Field Theory in Statistical Physics**, Dover (1975), section 21, Chapter 4.
¹⁶ R. Shankar, Physica **A 177**, 530 (1991) and Rev. Mod. Phys. **66**, 129 (1994).
¹⁷ Y. B. Kim, A. Furusaki, X. G. Wen and P. A. Lee, unpublished.
¹⁸ J. Polchinski, unpublished.
¹⁹ B. L. Altshuler, A. G. Aronov, p. 1 in **Electron-Electron interactions in disordered systems**, eds. A. L. Efros and M. Pollak, North-Holland (1985).
²⁰ I. E. Dzyaloshinsky and A. I. Larkin, Sov. Phys. JETP, **38**, 202 (1974).
²¹ P. B. Littlewood, J. Zaanen, G. Aeppli and H. Monien, Phys. Rev. **B 48**, 487 (1993).
²² A. J. Millis, p. 198 in **High Temperature Superconductivity: Proceedings**, eds. K. S. Bedell, D. Coffey, D. E. Meltzer, D. Pines, and J. R. Schrieffer, Addison-Wesley (Reading, CA: 1990).

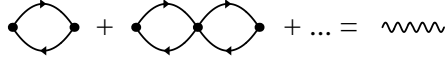


Fig 1

FIG. 1. RPA sum of bubble diagrams leading to dressed gauge field propagator (denoted by thick wavy line). The solid lines with arrows denote fermion propagators and the heavy dots denote the bare gauge field propagator. Whether the fermion propagators are bare or renormalized does not affect the result of the calculation.

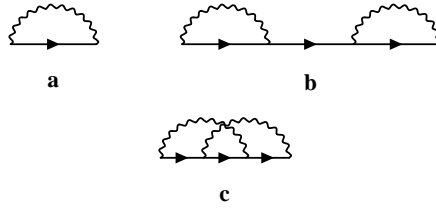


Fig 2

FIG. 2. Fermion self energy diagrams. The wavy line denotes the gauge field propagator (2) and the solid line the fermion propagator.

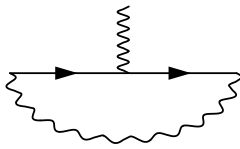


Fig 3

FIG. 3. Correction to fermion-gauge field vertex. The wavy line denotes the gauge field propagator (2) and the solid line the fermion propagator.

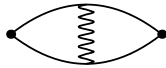


Fig 4

FIG. 4. Correction to fermion polarizability. The wavy line denotes the gauge field propagator (2) and the solid line the fermion propagator.

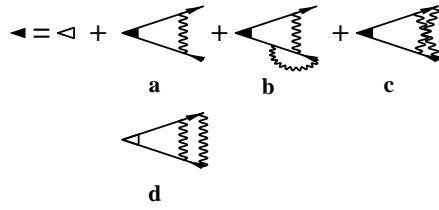


Fig 5

FIG. 5. Ladder sum giving renormalization of fermion $2p_F$ vertex Γ_{2p_f} (shaded triangle). a. Leading order in $\ln[N]/N$ b. and c. Subleading order in $1/N$. d. The leading order in $(\ln[N]/N)^2$. The heavy dot indicates the bare $2p_F$ vertex, the wavy line denotes the gauge field propagator (2) and the solid line the fermion propagator.



Fig 6

FIG. 6. Ladder sums giving renormalization of fermion $2p_F$ polarizability. Notation is the same as in Fig. 5

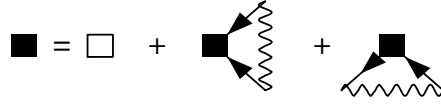


Fig 7

FIG. 7. Diagrams leading to renormalization group equation for short range fermion vertex W (heavy square). The wavy line denotes the gauge field propagator (2) and the solid line the fermion propagator.

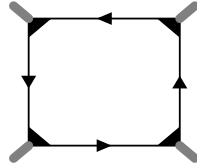


Fig 8

FIG. 8. Diagram leading to a singular interaction between spin waves. Solid lines denote fermion propagators, shaded triangles Γ_{2p_F} vertex.

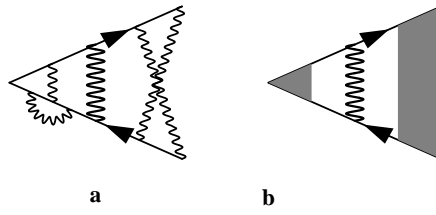


Fig 9

FIG. 9. a. Typical high order diagram for Γ^\perp . b. Sum of these diagrams. Broad wavy line represents propagator $k_\perp D(\omega, k_\perp)$ with large momentum transfer in perpendicular direction.